Journal of Solid State Chemistry 182 (2009) 2191–2201

Contents lists available at ScienceDirect

Journal of Solid State Chemistry

journal homepage: www.elsevier.com/locate/jssc

Mild hydrothermal synthesis, crystal structure, spectroscopic and magnetic properties of the $[M_x^{II}M_{2.5-x}^{III}(H_2O)_2(HP^{III}O_3)_y(P^{V}O_4)_{2-y}F]$ [M = Fe, $x = 2.08$, $y = 1.58$; M = Co, Ni, $x = 2.5$, $y = 2$] compounds

Joseba Orive [a], José L. Mesa [b,*], Estibaliz Legarra [c], Fernando Plazaola [c], María I. Arriortua [a], Teófilo Rojo [b]

[a] Departamento de Mineralogía y Petrología, Facultad de Ciencia y Tecnología, Universidad del País Vasco/EHU, Apdo. 644, E-48080 Bilbao, Spain
[b] Departamento de Química Inorgánica, Facultad de Ciencia y Tecnología, Universidad del País Vasco/EHU, Apdo. 644, E-48080 Bilbao, Spain
[c] Departamento de Electricidad y Electrónica, Facultad de Ciencia y Tecnología, Universidad del País Vasco/EHU, Apdo. 644, E-48080 Bilbao, Spain

ARTICLE INFO

Article history:
Received 10 February 2009
Received in revised form
26 May 2009
Accepted 28 May 2009
Available online 3 June 2009

Keywords:
Hydrothermal synthesis
Crystal structure
Thermal behavior
IRUV/Vis and Mössbauer spectroscopies
Magnetic measurements

ABSTRACT

The $[M_x^{II}M_{2.5-x}^{III}(H_2O)_2(HP^{III}O_3)_y(P^{V}O_4)_{2-y}F]$ [M = Fe (**1**), $x = 2.08$, $y = 1.58$; M = Co (**2**), $x = 2.5$, $y = 2$; Ni (**3**), $x = 2.5$, $y = 2$] compounds have been synthesized using mild hydrothermal conditions at 170 °C during five days. Single-crystals of (**1**) and (**2**), and polycrystalline sample of (**3**) were obtained. These isostructural compounds crystallize in the orthorhombic system, space group *Aba*2, with $a = 9.9598(2)$, $b = 18.8149(4)$ and $c = 8.5751(2)$ Å for (1), $a = 9.9142(7)$, $b = 18.570(1)$ and $c = 8.4920(5)$ Å for (2) and $a = 9.8038(2)$, $b = 18.2453(2)$ and $c = 8.4106(1)$ Å for (**3**), with $Z = 8$ in the three phases. An X-ray diffraction study reveals that the crystal structure is composed of a three-dimensional skeleton formed by $[MO_5F]$ and $[MO_4F_2]$ (M = Fe, Co and Ni) octahedra and $[HPO_3]$ tetrahedra, partially substituted by $[PO_4]$ tetrahedra in phase (**1**). The IR spectra show the vibrational modes of the water molecules and those of the $(HPO_3)^{2-}$ tetrahedral oxoanions. The thermal study indicates that the limit of thermal stability of these phases is 195 °C for (**1**) and 315 °C for (**2**) and (**3**). The electronic absorption spectroscopy shows the characteristic bands of the Fe(II), Co(II) and Ni(II) high-spin cations in slightly distorted octahedral geometry. Magnetic measurements indicate the existence of global antiferromagnetic interactions between the metallic centers with a ferromagnetic transition in the three compounds at 28, 14 and 21 K for (**1**), (**2**) and (**3**), respectively. Compound (**1**) exhibits a hysteresis loop with remnant magnetization and coercive field values of 0.72 emu/mol and 880 Oe, respectively.

1. Introduction

Materials science has been growing very fast in recent decades, giving rise to an incredible number of new phases with an amazing chemical diversity. The design of condensed phases, which can give rise to original physical properties (spectroscopic, magnetic,…), by making use of the great number of different cations and arrangement that they can exhibit, is an important area in this field [1,2]. In addition, mild hydrothermal synthesis can be used to obtain new phases that only exist in narrow stabilization ranges [3].

Since Bonavia et al. obtained the first organically template phosphite with open framework [4], the phosphite oxoanion $(HPO_3)^{2-}$, has been the source of many hybrid inorganic–organic phosphites [5]. Condensed phosphites, however, are scarce compared with the number of organically templated structures contained in this group. Cations used to synthesize these compounds are diverse and range from alkali metals to group 14 of the periodic table through transition metals and there are even some examples with rare earth elements. Most of these condensed phases were reported in the 1980s and 1990s and were only studied structurally [6]. The high versatility of the phosphite group to form new structures is due to its pyramidal morphology, which allows it to display properties of both tetrahedral and triangular oxianionic groups. In addition, the incorporation of the F^- anion in the inorganic framework of these compounds, following the synthetic route opened by Keller et al. [7], makes possible the synthesis of original and not structurally related phases with those ones found in literature.

In this paper we present the hydrothermal synthesis, crystal structure determination and the thermal, spectroscopic and magnetic behavior of three new inorganic fluoro-phosphites with a condensed crystal structure, one of them exhibiting a mixed valent Fe(II)/Fe(III) and $(HP^{III}O_3)^{2-}/(P^{V}O_4)^{3-}$ state.

* Corresponding author. Fax: +34 946013500.
E-mail address: joseluis.mesa@ehu.es (J.L. Mesa).

0022-4596/$ - see front matter © 2009 Elsevier Inc. All rights reserved.
doi:10.1016/j.jssc.2009.05.041

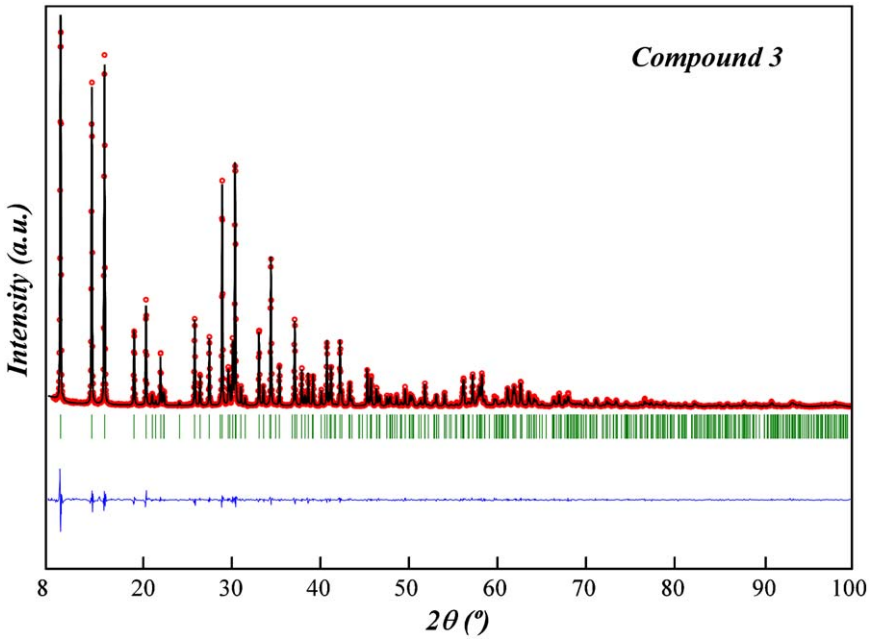

Fig. 1. Observed, calculated and difference X-ray powder diffraction pattern of (**3**).

2. Experimental section

2.1. Synthesis and characterization

The $Fe^{II}_{2.08}Fe^{III}_{0.42}(H_2O)_2(HP^{III}O_3)_{1.58}(P^{V}O_4)_{0.42}F$ (**1**) and $M_{2.5}(H_2O)_2(HP^{III}O_3)_2F$ [M = Co (**2**), Ni (**3**)] phases were synthesized under mild hydrothermal conditions. H_3PO_3 [7.50 mmol for (**1**), (**2**) and (**3**)], $Fe_2(SO_4)_3 \cdot 5H_2O$ (0.5625 mmol), $CoCl_2.6H_2O$ (0.75 mmol) and $NiCl_2 \cdot 6H_2O$ (0.9375 mmol) were dissolved in distilled water (30 mL) for (**1**) and (**2**) and in a mixture of 10 mL distilled water–20 mL butanol for (**3**). Then, 0.5 mL (13.9 mmol) of HF was added to the resulting solutions and finally the pH was increased in all cases to approximately 4, using 2-methyl-pipezazine. These reaction mixtures were sealed in PTFE-lined stainless steel pressure vessels. After five days at 170 °C, the vessels were slowly cooled to room temperature. Three different products with gray, pink or yellow color for (**1**), (**2**) and (**3**), respectively, were obtained, and then they were isolated by filtration, washed with water and acetone and dried over P_2O_5 for 1 h.

The compositions of the products were calculated with ICP-AES spectroscopy. The amount of the fluoride anion was calculated by using a selective electrode. $Fe^{II}_{2.08}Fe^{III}_{0.42}(H_2O)_2(HP^{III}O_3)_{1.58}(P^{V}O_4)_{0.42}F$ (**1**). Calc: P, 17.1; Fe, 38.7; F, 5.3. Found: P, 16.8(2); Fe, 38.3(2); F, 5.1(1). $Co_{2.5}(H_2O)_2(HP^{III}O_3)_2F$ (**2**). Calc: P, 17.3; Co, 40.7; F, 5.2. Found: P, 17.0(1); Co, 40.5(1); F, 5.1(1).). $Ni_{2.5}(H_2O)_2(HP^{III}O_3)_2F$ (**3**). Calc: P, 17.2; Ni, 40.6; F, 5.2. Found: P, 17.0(1); Ni, 40.2(1); F, 5.0(1). The densities measured in a mixture of diiodomethane (CH_2I_2, $\rho = 3.325\,g/cm^3$) and chloroform (Cl_3CH, $\rho = 1.492\,g/cm^3$), are 2.965(2), 3.020(2) and 3.156(3) g/cm^3, for (**1**), (**2**) and (**3**), respectively.

2.2. Single crystal X-ray diffraction study

Prismatic single crystals with dimensions $0.25 \times 0.14 \times 0.02$ and $0.35 \times 0.14 \times 0.01$ mm for (**1**) and (**2**), respectively, were selected under a polarizing microscope and mounted on a glass fiber. Single-crystal X-ray diffraction data were collected at room temperature on an Oxford Diffraction XCALIBUR2 and a STOE IPDS automated diffractometers (Mo-$K\alpha$ radiation) both equipped with a CCD detector, for compounds (**1**) and (**2**), respectively. The Lorentz-polarization and absorption corrections were made with the diffractometer softwares, taking into account the size and shape of the crystals. The crystal structure of (**1**) was solved by

Table 1
Crystallographic data and structure refinement parameters for **(1)** and **(2)**.

Formula	$Fe^{II}_{2.08}Fe^{III}_{0.42}(H_2O)_2(HP^{III}O_3)_{1.58}(P^{V}O_4)_{0.42}F$	$Co_{2.5}(H_2O)_2(HP^{III}O_3)_2F(P^{V}O_4)_{0.42}F$
Molecular weight (g/mol)	358.48	358.28
Crystal system	Orthorhombic	Orthorhombic
Space group (N° 41)	*Aba*2	*Aba*2
a (Å)	9.9598(2)	9.9142(7)
b (Å)	18.8149(4)	18.570(1)
c (Å)	8.5751(2)	8.4920(5)
V (Å^3)	1606.91(6)	1563.4(2)
Z	8	8
ρ_{obs}, ρ_{calc} (g/cm^3)	2.965(2), 2.964	3.020(2), 3.044
F(000)	1404	1380
Temperature (K)	293(2)	293(2)
Diffractometer	Oxford Diffraction Xcalibur2	STOE IPDS
μ (mm^{-1})	4.917	5.709
Radiation λ(Mo $K\alpha$) (Å)	0.71073	0.71073
Limiting indices (h, k, l)	$h \pm 12$, $k \pm 9$, $l \pm 10$	$h \pm 12$, $k \pm 9$, $l \pm 10$
Theta range (°)	2.98–26.37	3.01–26.37
N. reflections (indep.)	14049	5477
N. reflections (obs.)	1633	1572
R (int.)	0.0398	0.0604
R [$I>2\sigma(I)$]	$R_1 = 0.0227$, $wR_2 = 0.05221$	$R_1 = 0.0302$, $wR_2 = 0.0603$
R [all data]	$R_1 = 0.0265$, $wR_2 = 0.05431$	$R_1 = 0.0368$, $wR_2 = 0.0612$
G.O.F	1.03	1.091
Max. and min. e. density (e/Å^3)	0.829, −0.391	0.464, −0.625

$R_1 = [(|F_0|-|F_c|)]/|F_0|$; $wR_2 = [[w(|F_0|^2-|F_c|^2)^2]/[w(|F_0|^2)^2]]^{1/2}$; $w = 1/[\sigma^2|F_0|^2 + (xp)^2 + yp]$; where $p = [|F_0|^2 + 2|F_c|^2]/3$; $x = 0.0357$, $y = 0.00$ for (**1**) and $x = 0.0347$, $y = 0.00$ for (**2**).

direct methods, SHELXS 97 computer program [8] and refined by full matrix least-squares based on F^2, using the SHELXL 97 [9] in the acentrosymmetric *C2cb* orthorhombic space group. At the end of this procedure was find a residual electronic density of three electrons was found at a distance of approximately 1.51 Å around every phosphorous atom. These residual electronic densities are very high to be considered as belonging to hydrogen atoms of the P(1) and P(2) atoms of the phosphite groups. So the possibility of the simultaneous existence of $(HPO_3)^{2-}$ and $(PO_4)^{3-}$ anions was considered. In order to solve this problem a disordered system was created: O(10), H(10) on the P(1) tetrahedron and O(11), H(11) on the P(2) tetrahedron, that was studied with the PART option [10] belonging to the SHELXL 97 program [9]. The final percentage of occupancy obtained for this disordered system was 25.4% O(10) and 74.6% H(10) on the P(1) and 13.9% O(11), 86.1% H(11) on P(2). This result allows us to conclude the existence of $(HPO_3)^{2-}$ and $(PO_4)^{3-}$ anions in the crystal structure of (**1**). Finally, the positions of the hydrogen atoms of the water molecules were located in the Fourier map, and the space group was changed to the *Aba2* standard one using the PLATON option [11] of the WinGX. In addition, the electroneutrality of the chemical formula required the existence of a mixed valence for the iron atoms, corroborated by the Mössbauer study. The final formula proposed for (**1**) is $Fe^{II}_{2.08}Fe^{III}_{0.42}(H_2O)_2(HP^{III}O_3)_{1.58}(P^{V}O_4)_{0.42}F$. As the spatial group is non-centrosymmetric, the Flack parameter was studied in order to determine the absolute structure, after inversion of the structure the value obtained for BASF was 0.68(2).

Taking into account the similar unit cell of compound (**2**) with that of (**1**), the crystal structure of this first phase was solved with the isomorphic substitution method, after corroborating the non-existence of $(PO_4)^{3-}$ anions in its chemical composition, because the residual electronic density around P(1) and P(2), at approximately 1.33 Å, corresponds to the hydrogen atoms of the phosphite anions. The BASF parameter was 0.19(4). On the basis of this results, the chemical formula for (**2**) is $Co_{2.5}(H_2O)_2(HP^{III}O_3)_2F$, in which the cobalt cation exhibits an oxidation state of +2.

Table 2
Bond distances (Å) and angles (°) for **(1)**.

Octahedron [Fe(1)O_5F]						
Fe(1)	O(1)	F(1)	O(2)	O(6)	O(3)	O(5)
O(5)	78.1(1)	89.15(9)	84.6(1)	91.70(1)	175.40(1)	2.226(3)
O(3)	99.2(1)	93.67(9)	91.8(1)	92.60(1)	2.143(3)	
O(6)	98.9(1)	78.04(9)	164.8(1)	2.126(3)		
O(2)	94.7(1)	87.1(1)	2.110(4)			
F(1)	166.9(1)	2.106(3)				
O(1)	2.083(3)					
Octahedron [Fe(2)O_5F]						
Fe(2)	O(5)	O(3)^{iv}	F(1)^{vi}	O(6)^{vi}	O(9)	O(1)
O(1)	78.2(1)	175.4(1)	86.65(9)	94.6(1)	84.3(1)	2.235(3)
O(9)	92.2(2)	92.3(1)	89.1(1)	166.6(1)	2.150(4)	
O(6)^{vi}	100.7(1)	89.4(1)	77.5(1)	2.132(3)		
F(1)^{vi}	164.6(1)	96.4(9)	2.124(3)			
O(3)^{iv}	98.90(1)	2.117(3)				
O(5)	2.068(3)					
Octahedron [Fe(3)O_4F_2]						
Fe(3)	O(7)	O(7)^{v}	O(8)^{viii}	O(8)^{vii}	F(1)^{v}	F(1)
F(1)	90.1(1)	92.0(1)	92.5(1)	85.3(1)	177.0(2)	2.130(2)
F(1)^{v}	92.0(1)	90.1(1)	85.3(1)	92.5(1)	2.130(2)	
O(8)^{vii}	94.1(1)	176.70(2)	84.1(2)	2.085(4)		
O(8)^{viii}	176.70(2)	94.1(1)	2.085(4)			
O(7)^{v}	87.9(2)	2.072(3)				
O(7)	2.072(3)					
Tetrahedra [HP(1)O_3]/[P(1)O_4]						
P(1)	O(10)	O(5)^{vi}	O(6)^{iii}	O(1)	H(10)	
H(10)	17(4)	95(5)	119(4)	197(4)	1.30(1)	
O(1)	108.0(7)	111.5(2)	111.9(2)	1.528(3)		
O(6)^{iii}	103.4(6)	112.4(2)	1.524(2)			
O(5)^{vi}	109.3(8)	1.518(3)				
O(10)	1.498(8)					
Tetrahedra [HP(2)O_3]/[P(2)O_4]						
P(2)	O(11)	O(8)	O(7)	O(3)	H(11)	
H(11)	8(1)	108.1(6)	107.2(6)	106.2(6)	1.30(1)	
O(3)	113(1)	112.0(2)	112.6(2)	1.536(3)		
O(7)	101(1)	110.5(2)	1.522(4)			
O(8)	107(1)	1.506(4)				
O(11)	1.50(1)					

The O(10) and O(11) are the oxygen atoms of the phosphate groups.
Symmetry codes: i = $x-1/2, -y+3/2, z$; ii = $-x, -y+3/2, z+1/2$; iii = $-x, -y+1, z$; iv = $x-1/2, -y+1, z-1/2$; v = $-x+1/2, y, z-1/2$; vi = $x+1/2, -y+3/2, z$; vii = $-x, -y+3/2, z-1/2$; and viii = $-x+1/2, y, z+1/2$.

Table 3
Bond distances (Å) and angles (°) for **(2)**.

Octahedron [Co(1)O_5F]						
Co(1)	O(1)	F(1)	O(2)	O(6)	O(3)	O(5)
O(5)	78.8(2)	89.3(2)	86.0(2)	91.4(2)	174.4(2)	2.186(6)
O(3)	97.4(2)	94.8(2)	90.3(3)	93.1(2)	2.119(7)	
O(6)	97.1(2)	78.7(2)	167.0(2)	2.086(6)		
O(2)	94.9(2)	88.5(2)	2.048(7)			
F(1)	167.3(2)	2.078(5)				
O(1)	2.082(6)					
Octahedron [Co(2)O_5F]						
Co(2)	O(5)	O(3)^{ii}	F(1)^{i}	O(6)^{i}	O(9)	O(1)
O(1)	79.4(2)	174.8(2)	86.8(2)	94.6(2)	83.1(2)	2.190(5)
O(9)	92.1(3)	92.8(3)	89.2(2)	167.0(2)	2.187(7)	
O(6)^{i}	100.0(2)	90.0(2)	77.9(2)	2.119(6)		
F(1)^{i}	165.9(2)	96.5(2)	2.083(5)			
O(3)^{ii}	97.5(2)	2.088(7)				
O(5)	2.045(6)					
Octahedron [Co(3)O_4F_2]						
Co(3)	O(7)	O(7)^{v}	O(8)^{iii}	O(8)^{iv}	F(1)^{v}	F(1)
F(1)	90.2(2)	92.5(2)	92.0(2)	85.2(2)	176.2(3)	2.114(2)
F(1)^{v}	92.5(2)	90.2(2)	85.2(2)	92.0(2)	2.114(2)	
O(8)^{iv}	95.2(1)	177.0(3)	83.0(4)	2.064(7)		
O(8)^{iii}	177.0(3)	95.2(1)	2.064(7)			
O(7)^{v}	86.7(4)	2.071(6)				
O(7)	2.071(6)					
Tetrahedron [HP(1)O_3]						
P(1)	O(1)		O(5)^{i}	O(6)^{viii}		H(1)
H(1)	100(4)		111(4)	105(2)		1.30(1)
O(6)^{viii}	113.0(4)		111.8(4)	1.530(3)		
O(5)^{i}	111.2(2)		1.528(6)			
O(1)	1.517(6)					
Tetrahedron [HP(2)O_3]						
P(2)	O(3)		O(7)	O(8)		H(2)
H(2)	115(3)		94(3)	109(3)		1.30(1)
O(8)	112.9(4)		109.8(3)	1.517(6)		
O(7)	113.9(3)		1.514(6)			
O(3)	1.548(4)					

Symmetry codes: i = $-x$, $-y$+3/2, z+1/2; ii = x−1/2, $-y$+3/2, z; iii = x−1/2, $-y$+1, z−1/2; iv = $-x$+1/2, y+0, z−1/2; v = $-x$, $-y$+1, z; vi = x+1/2, $-y$+3/2, z; vii = $-x$,$-y$+3/2, z−1/2.

Finally, for phase (**3**), obtained as powdered sample, its pattern matching analysis was carried out through the Rietveld method, with the FULLPROF program [12]. The unit cell parameters of (**1**) were used in the structural refinement, obtaining a good agreement between the experimental and calculated diffractograms [$R_p = 9.14$, $Rw_p = 12.2$, $Rexp = 9.14$, $Chi2 = 1.78$ and $R_B = 0.042$] (Fig. 1). The refined cell parameters of (**3**) are $a = 9.8038(2)$, $b = 18.2453(2)$ and $c = 8.4106(1)$ Å and so the proposed chemical formula is $Ni_{2.5}(H_2O)_2(HP^{III}O_3)_2F$.

All structure drawings were made using the ATOMS Program [13]. The crystallographic data of the two phases solved from single-crystal data are given in Table 1. The selected bond distances and angles are reported in Tables 2 and 3.

2.3. Physicochemical characterization techniques

Thermogravimetric analyses were performed on an SDC 2960 simultaneous DSC-TGA TA instrument. Crucibles containing 20 mg of every sample were heated at a rate of 5 °C/min from room temperature to 800 °C. Temperature dependence X-ray diffraction experiments were carried out in argon atmosphere with a PHILIPS X'PERT automatic diffractometer (Cu $K\alpha$ radiation) equipped with a variable-temperature stage (Anton Paar HTK16) and a Pt sample holder. The IR spectra (KBr pellets) were obtained with a Nicolet FT-IR 740 spectrophotometer in the 400–4000 cm^{-1} range. Diffuse reflectance spectra were registered at room temperature on a Cary 2415 spectrometer in the 210–2000 nm range. Mössbauer spectra were obtained using a constant-acceleration Mössbauer spectrometer with a ^{57}Co/Rh source. Velocity calibration was done using a metallic Fe foil, and the Mössbauer spectral parameters are given relative to this standard at room temperature. The Mössbauer spectra were fitted with the NORMOS [14] program. Magnetic measurements on the powdered sample were performed in the temperature range 2.0–300 K for all compounds, at 0.1, 0.05 and 0.01 T using a Quantum Design MPMS-7 SQUID magnetometer. This value is in the range of linear dependence of magnetization vs magnetic field even at 5.0 K.

3. Results and discussion

3.1. Description of the structures

The crystal structures of compounds (**1**), (**2**) and (**3**) consist in a three-dimensional network formed by [MO_5F] and [MO_4F_2] (M = Fe, Co and Ni) octahedra and [HPO_3] tetrahedra, partially substituted by [PO_4] tetrahedra in phase (**1**) (Fig. 2). These elements give rise to two kind of layers, denoted as *a* and *b* (Fig. 3). The sheets type *a* are made up of [$M(3)O_4F_2$] octahedra linked through the O(7) and O(8) oxygen atoms of the [$HP(2)O_3$] phosphite pyramids, that in the case of phase (**1**) are partially substituted by [$P(2)O_4$] tetrahedra. The type *b* layers are formed by [$M(1)O_5F$] and [$M(2)O_5F$] edge-shared octahedra, which give rise to chains parallel to the [001] direction. These chains are linked by the O(3) oxygen atom, belonging simultaneously to the [$M(1)O_5F$] and [$M(2)O_5F$] octahedra, and by the O(5), O(6) and O(1) atoms of the [$HP(1)O_3$] phosphite and [$P(1)O_4$] phosphate anions. The layers type *a*,*a*′ and *b*,*b*′, shown in Fig. 2, are related through the translational mirrors and axes characteristic of the space group.

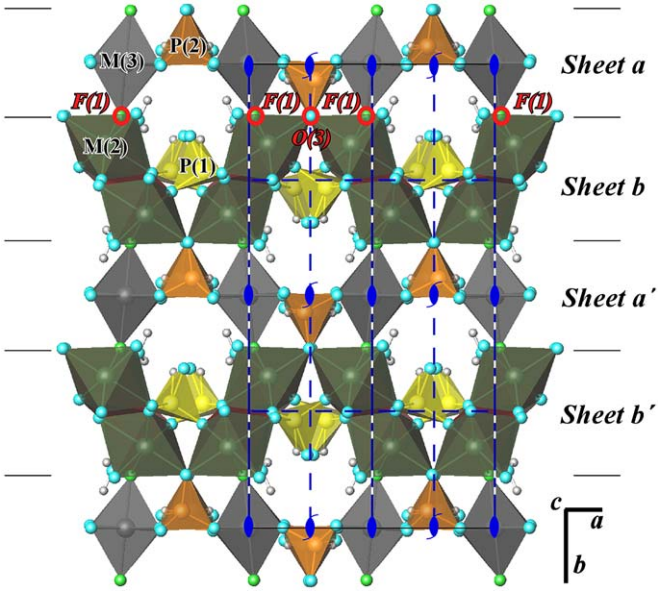

Fig. 2. Polyhedral view of the crystal structures showing the sheets along the [001] direction.

In the [$M(1)O_5F$] octahedra, the $M(1)$ positions are occupied by the divalent Fe(II) and Co(II) cations. The metal–oxygen bond distances range between 2.083(3)–2.226(3) Å for Fe(II) and between 2.048(7)–2.186(6) Å for Co(II), whereas the metal–fluor bond lengths are in the 2.106(3)–2.078(5) Å range for Fe(II) and Co(II). The [$M(2)O_5F$] octahedra exhibit M(II)–O bond distances ranging from 2.068(3) to 2.235(3) Å and from 2.045(6) to 2.190(5) Å for Fe(II) and Co(II), respectively. The M(II)–F bond lengths show values of 2.124(3) Å for Fe(II) and of 2.083(5) Å for Co(II). Finally, the [$M(3)O_4F_2$] octahedra of the phase (**1**) contain simultaneously Fe(II) and Fe(III) cations. The iron–O(7) and O(8) distances are 2.072(3) and 2.085(4) Å, respectively. The iron–fluor bond length is 2.130(2) Å. For phase (**2**), the metal–O bond distances in these [$M(3)O_4F_2$] polyhedra range from 2.064(7) to 2.071(6) Å for Co(II). The *cis*- and *trans*-bond angles show the typical values habitually found in slightly distorted octahedral environments (see Tables 2 and 3). The distortion of the [$M(1)O_5F$], [$M(2)O_5F$] and [$M(3)O_4F_2$] octahedra from the octahedral ideal symmetry, calculated with the Alvarez et al. method [15] using the SHAPE v1.1a program [16], are S(Oh) = 0.88. 0.98 and 0.20, respectively.

For (**1**) the P(1)–O and P(2)–O bond distances in the [$HP(1),(2)O_3$] and [$P(1),(2)O_4$] polyhedra range from 1.498(8) to 1.528(3) Å and from 1.50(1) to 1.536(3) Å, respectively, whereas the P(1)–H(1) and P(2)–H(2) lengths are of 1.30(1) Å. For (**2**) the P(1)–O(1) distances are in the range 1.517(6)–1.530(3), whereas the P(2)–O(2) bond lengths range from 1.514(6) to 1.548(4) Å. In these two phases the mean value of the P–H bond distance is 1.30(1) Å. The bond angles of these oxoanions are near to the ideal value of 109°, as is expected for a sp^3 hybridization of the phosphorous atom. The distortion of the [HPO_3] polyhedra from the tetrahedral symmetry has a mean value of 0.30(1), indicating a symmetry near to the ideal [15,16].

3.2. Thermal study

The thermogravimetric curves of the three phases (see Supplementary Material) show an initial mass loss of approximately 1% until 215, 200 and 275 °C, for (**1**), (**2**) and (**3**), which are

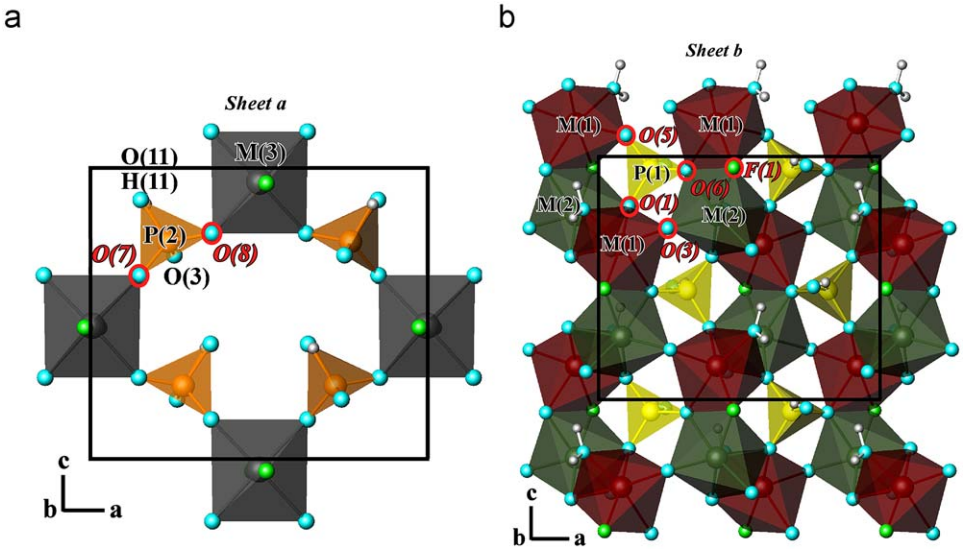

Fig. 3. Polyhedral view of the sheets "*a*" and "*b*".

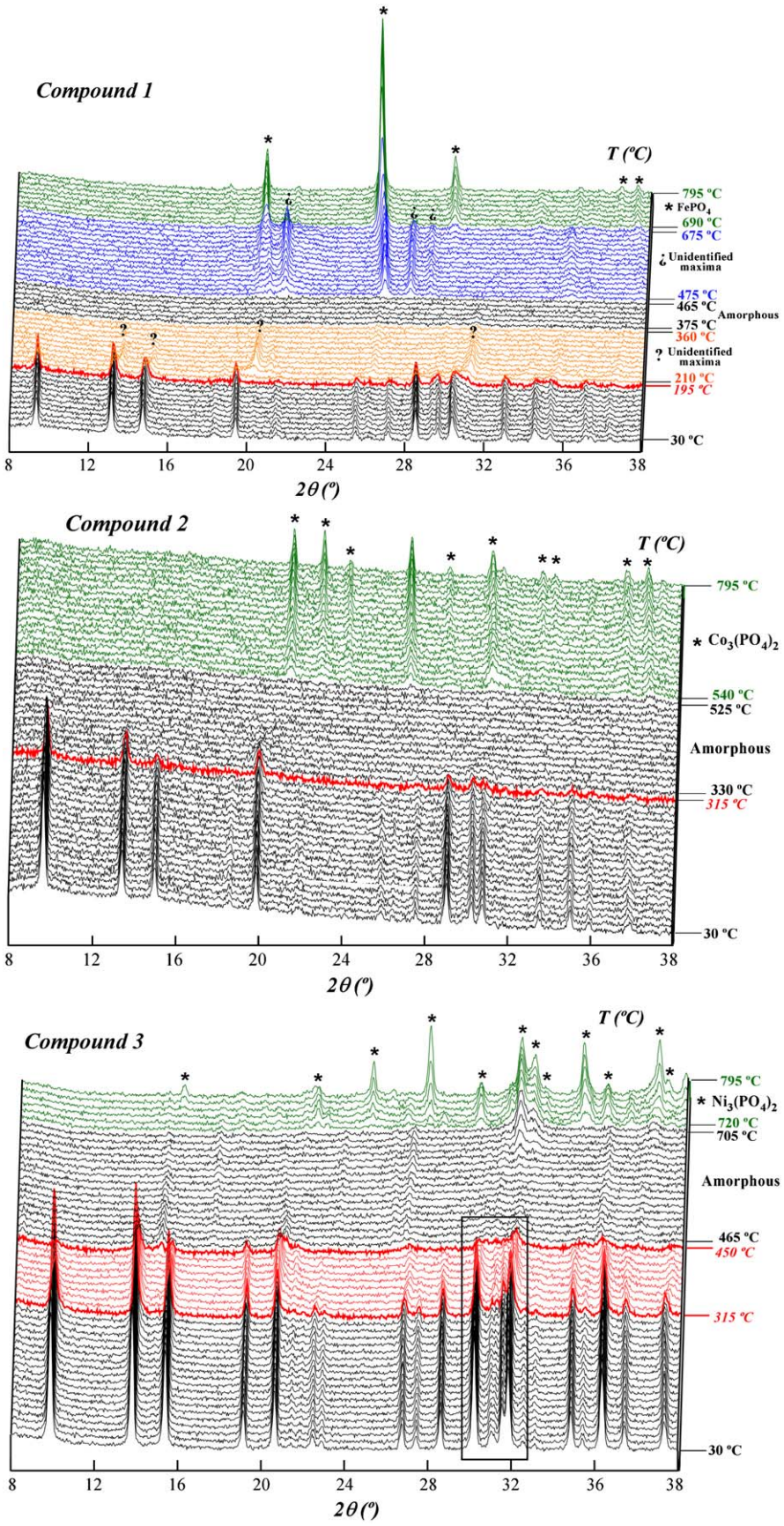

Fig. 4. Thermodiffractograms of compounds (**1**), (**2**) and (**3**).

attributed to the elimination of the water adsorbed by the compounds. Above these temperatures the decomposition of the phases starts, taking place in several superposed steps. From 230 to 415 °C for (**1**) the exothermic elimination of the two coordinated water molecules takes place and the elimination of the fluoride anions, as $F_2(g)$, in the 415–550 °C range being. For (**2**) these processes take place in the 75–630 °C range, whereas that for (**3**) the same decomposition occurs in the 255–550 °C range. In both phases (**2**) and (**3**) these mass looses take place as superimposed steps. At temperatures of 560, 630 and 600 °C for (**1**), (**2**) and (**3**), respectively, an exothermic peak is observed in the ATD curve, indicating the formation of inorganic residues, which are the $Fe(PO_4)$ [SG. $P3_12_1$, $a = 5.036$, $c = 11.255$ Å, $\gamma = 120°$] [17], $Co_3(PO_4)_2$ [S.G. $P2_1/n$, $a = 7.557(7)$, $b = 8.3736(6)$, $c = 5.0651(6)$ Å, $\beta = 94.03°$] [18] and $Ni_3(PO_4)_2$ [S.G. $P21/c$, $a = 5.830(2)$, $b = 4.700(2)$, $c = 10.107(4)$ Å, $\beta = 91.22(2)°$] [19].

The thermal behavior of the three compounds was also studied by using time-resolved X-ray thermodiffractometry in air. A Bruker D8 Advance diffractometer (Cu-$K\alpha$ radiation) equipped with, a variable-temperature stage (Paar Physica TCU2000), a Pt sample heater and a Vanter high-speed one dimensional detector with three degrees of angular aperture, were used in the experiment. The power patterns were recorded in the $8° \leq 2\theta \leq 38°$ range, counting 1 min/diffractogram and increasing the temperature at 10 °C/min from room temperature to 795 °C (Fig. 4). The thermodiffractograms remain unchanged until 195 °C for (**1**) and 315 °C for (**2**) and (**3**), indicating these temperatures the limit of thermal stability of the phases. For (**1**), above 475 °C and until 675 °C several diffraction maxima appear that cannot be identified with phases of the PDF file. At the latter temperature begins the crystallization of the $Fe(PO_4)$ inorganic residue that remains until the final temperature of the experiment. For (**2**), at temperatures higher than 315 °C and until 525 °C there exists an amorphous phase, with 540 °C the temperature at which the crystallization of $Co_3(PO_4)_2$ starts. Finally, for (**3**) in the 315–450 °C range the thermodiffractograms show the existence of this phase and in the 465–705 °C range, several diffraction maxima, not identified with phases of the PDF file, were observed. At temperatures above 720 °C the $Ni_3(PO_4)_2$ crystallizes. The inorganic phosphates obtained as residues in the thermodiffractometric study are the same than those obtained in the thermogravimetric one.

The thermal expansion coefficients for the three compounds have been calculated from the data obtained of the thermodiffractometry, using the expression $V(T) = VTr\exp[\alpha_0(T-Tr)]$ [20], in which VTr is the initial room temperature and α_0 the thermal expansion coefficient. The results are shown in Table 4 and the plots of these results are given as Supplementary Material.

Table 4
Thermal expansion coefficients of the parameters and volume of the unit-cells for (**1**), (**2**) and (**3**).

	Compound (**1**)	Compound (**2**)	Compound (**3**)
α_0 a (°C^{-1})	5.0×10^{-6}	1.1×10^{-5}	6.0×10^{-6}
α_0 b (°C^{-1})	1.6×10^{-5}	1.1×10^{-5}	1.3×10^{-5}
α_0 c (°C^{-1})	2.5×10^{-5}	2.1×10^{-5}	1.8×10^{-5}
α_0 V (°C^{-1})	4.5×10^{-5}	4.5×10^{-5}	3.8×10^{-5}

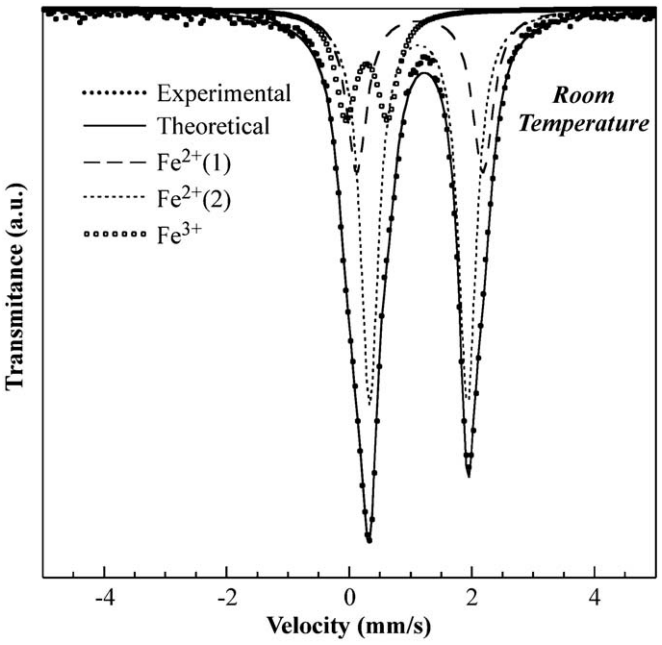

Fig. 5. Mössbauer spectrum of (**1**) at room temperature.

Table 5
Hyperfine parameters from fitting of the Mössbauer spectrum of (**1**) at 300 K.

Position	δ (mm/s)	ΔE (mm/s)	Oxidation state	Atoms per cell	%Fe
Fe(1)	1.151(2)	2.058(6)	2+	8	83.00
Fe(2)	1.1309(7)	1.594(3)	2+	8	
Fe(3)	0.282(3)	0.680(6)	3+	4	17.00

3.3. Infrared, UV-Vis and Mössbauer spectroscopies

IR spectra of (**1**), (**2**) and (**3**) exhibit the bands corresponding to the vibrations of the water molecules and the $(HPO_3)^{2-}$ phosphite oxoanions. In the three phases, the stretching ν(O–H) and deformation δ(O–H) modes belonging to the water molecules appear at 3500 and 1640 cm^{-1}. Around 2500 cm^{-1}, two bands corresponding to the stretching vibrational mode, ν(P–H), of the phosphite can be observed in the spectra. The presence of these two bands is in good agreement with the existence of two crystallographically independent phosphite anions [21]. At lower frequencies, approximately 1100, 1015 and 975 cm^{-1}, appear the bands corresponding to asymmetrical stretching $\nu_{as}(PO_3)$, deformation δ(PH) and symmetrical stretching $\nu_s(PO_3)$ modes of $(HPO_3)^{2-}$ anion, respectively. Finally, the symmetrical and antisymmetrical deformation vibrations, $\delta_s(PO_3)$ and $\delta_{as}(PO_3)$ are detected at approximately 575 and 500 cm^{-1}, respectively.

In the diffuse reflectance spectrum of (**1**) two bands at approximately 7200 and 9700 cm^{-1} are observed. These bands are characteristic of the iron(II) d^6-high spin cation in a slightly distorted octahedral environment. The bands correspond to the electronic transitions from the $^5T_{2g}(^5D)$ fundamental state to the excited level $^5E_{2g}(^5D)$ that is splitted as a consequence of the existence of non-regular [Fe(1), Fe(2)O_5F] and [Fe(3)O_4F_2] octahedra. The energy associated with this transition corresponds, according to the Tanabe–Sugano diagram [22,23], to the Dq parameter. The value obtained is $Dq = 845$ cm^{-1}. These results are in good agreement with the values observed in other related compounds containing this cation [24]. In the spectrum an intense band can also be observed at approximately 17 500 cm^{-1}. This band could be tentatively assigned to the intervalence transitions between the Fe^{2+} and Fe^{3+} cations, because their polyhedra share the oxygen and fluoride anions and the intermetallic bond distance is sufficiently short (approximately 3.2 Å).

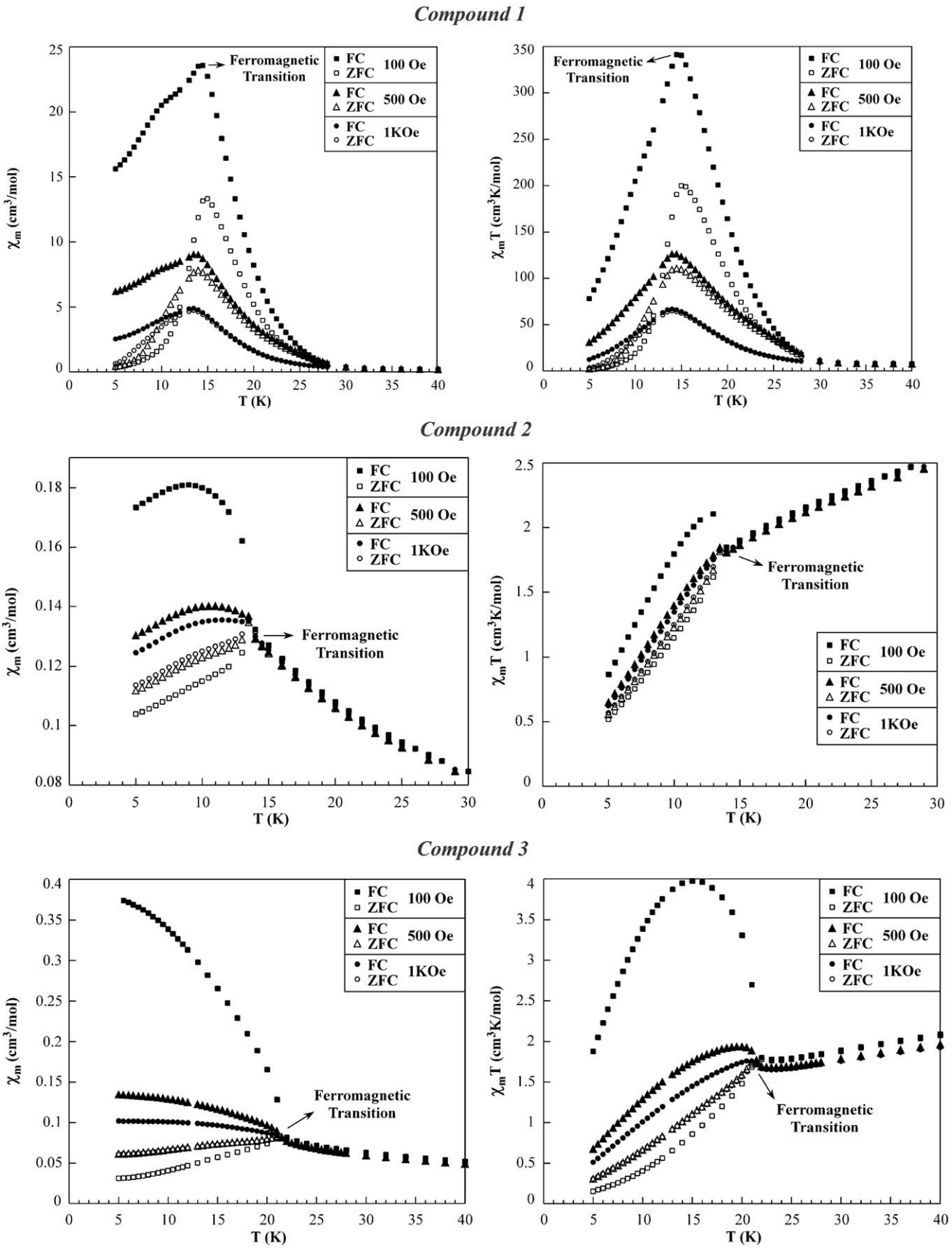

Fig. 6. Thermal evolution of the χ_m and $\chi_m T$ curves for compounds (**1**), (**2**) and (**3**).

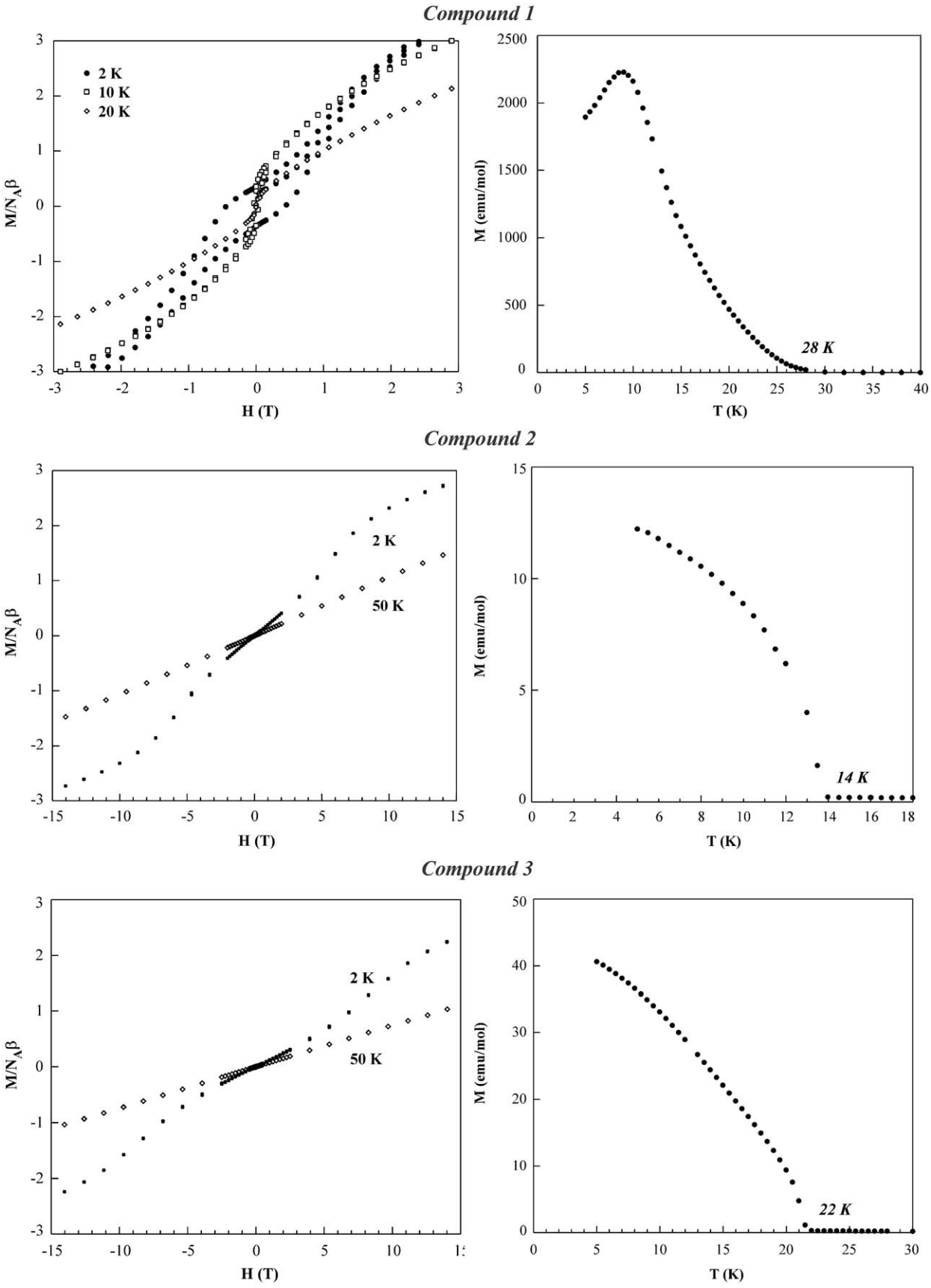

Fig. 7. Hysteresis loops and remnant magnetization of compounds (**1**), (**2**) and (**3**).

In the case of phase (**2**), the diffuse reflectance spectrum shows bands at approximately 6950, 13 695 and 20 560 cm^{-1}. These bands have been assigned to the allowed transitions from the $^4T_{1g}(^4F)$ fundamental state to the excited levels $^4T_{2g}(^4F)$, $^4A_{2g}(^4F)$ and $^4T_{1g}(^4P)$ for the Co(II) d^7-cation in a slightly distorted octahedral environment [22,23]. The shoulder observed at approximately 7550 has been assigned to the forbidden transition between the $^4T_{1g}(^4F)$ state and the excited $^2E_{1g}(^2G)$ level. The calculated values of the *Dq*, *B* and *C* parameters are 675, 895 and 3735 cm^{-1}. These results are in the range habitually found for the octahedrically coordinated Co(II) cation [24]. The reduction of the *B*-parameter value with respect to that of the free ion (1115 cm^{-1}) suggests a significant covalence in the Co–O/F bonds.

The diffuse reflectance spectrum of (**3**) exhibits the essential characteristic of octahedral coordinated Ni(II) compounds. Two absorption bands ascribed to the spin allowed transitions $^3A_{2g}(^3F)\rightarrow{}^3T_{2g}(^3F)$ and $^3T_{1g}(^3F)$ are observed at frequencies of 7200 and 20 200 cm^{-1}. The spin forbidden transitions $^3A_{2g}(^3F)\rightarrow{}^1E_g(^1D)$ and $^1T_{2g}(^1D)$ can be observed at 13 900 and 24 500 cm^{-1}. The *Dq* and *Racah* (*B* and *C*) parameters were calculated by fitting the experimental frequencies to an energy level diagram for octahedral d^8-system [22,23]. The values obtained are $Dq = 720$, $B = 680$ and $C = 4730$ cm^{-1}. The B-value is approximately 70% that of the free cation (1030 cm^{-1}).

The Mössbauer spectrum of (**1**), carried out at room temperature (298 K), is shown in Fig. 5. The spectrum has been fitted by using three doublets. Two of them correspond to the two crystallographically independent Fe(II) cations, and the third one corresponds to the existence of an amount of Fe(III) in the structure of this phase. The values of the isomer shift and quadrupolar splitting parameters are given in Table 5 for every kind of iron cation, together with the percentage of this element on the different positions occupied in the crystal structure.

3.4. Magnetic behavior

The magnetic susceptibility of the three phases has been measured on powdered samples from room temperature to 5 K, in the zero field cooling (ZFC) and field cooling (FC) modes, at 1000, 500 and 100 Oe (Fig. 6).

The molar magnetic susceptibility of (**1**), (**2**) and (**3**) increases continuously from 300 to 30 K, due to the temperature-depended paramagnetism. From 30 K, both the ZFC and FC curves show an abrupt increase until approximately 15 K and then they decrease continuously until 5 K. The susceptibility follows the Curie–Weiss law above 50, 25 and 30 K for (**1**), (**2**) and (**3**), respectively, with values of the Curie and Curie–Weiss temperature of $Cm = 10.00$ cm^3 K/mol (**1**), 5.72 (**2**) and 3.40 (**3**) and $\theta = -20.7$ K (**1**), −42.7 (**2**) and −33.1 (**3**). These results and the continuous decrease of the $\chi_m T$ vs *T* curves indicate a global antiferromagnetic behavior for the three compounds.

The susceptibility measurements carried out at 500 and 100 Oe for the three phases show irreversibility when they are performed in the ZFC and FC modes (see Fig. 6). This result suggests the existence of weak ferromagnetic components at low temperatures, in good agreement with the abrupt increase of the χ_m vs *T* curve observed in the 30–15 K range.

In order to corroborate the existence of these ferromagnetic components in the phases, magnetization measurements at different magnetic fields were performed (Fig. 7). It was found that, compound (**1**) exhibits a hysteresis loop at 2 K, with values of the remnant magnetization and coercive field of 0.72 emu/mol and 880 Oe, respectively. However, compounds (**2**) and (**3**) do not show hysteresis loops. In addition, the remnant magnetization was evaluated cooling samples of the three phases in presence of a magnetic field of 100 Oe and then heating ones, after eliminating the magnetic field. These measurements show that the magnetization disappears at temperatures of 28, 14 and 21 K for (**1**), (**2**) and (**3**), respectively. These results confirm the existence of weak ferromagnetic components in the three phases, probably due to spin canting phenomena.

4. Concluding remarks

Three new inorganic fluoro-phosphites, one of them with mixed valent Fe(II)/Fe(III) and $(HP^{III}O_3)^{2-}/(P^{V}O_4)^{3-}$, have been synthesized by mild hydrothermal techniques. The isostructural compounds show a three dimensional structure formed by $[MO_5F]$ and $[MO_4F_2]$ (M = Fe, Co and Ni) octahedra and $[HPO_3]$ tetrahedra, partially substituted by $[PO_4]$ tetrahedra in the mixed valent phase. The diffuse reflectance measurements confirm the octahedral geometry of the metallic cations and their oxidation states. Magnetization measurements are consistent with the existence of major antiferromagnetic interactions, and a ferromagnetic transition probably due to a spin canting phenomenon in the 15–30 K range.

Acknowledgments

This work has been financially supported by the "Ministerio de Educación y Ciencia" (MAT2007-60400/66737-C02-01) and the "Gobierno Vasco" (IT-177-07 and GIC07/126-IT-312-07). The authors thank the technicians of SGIker, Dr. I. Orue, Dr. F.J. Sangüesa, Dr. A. Larrañaga and Dr. P. Vitoria, financed by the National Program for the Promotion of Human Resources within the National Plan of Scientific Research, Development and Innovation, "Ministerio de Ciencia y Tecnología" and "Fondo Social Europeo" (FSE), for the magnetic measurements and the X-ray diffraction measurement, respectively. J. Orive wishes to thank the "Departamento de Investigación y Ciencia del Gobierno Vasco/Eusko Jaurlaritza" for funding.

Appendix A. Supplementary material

Supplementary data associated with this article can be found in the online version at doi:10.1016/j.jssc.2009.05.041.

References

[1] S.M. Kauzlarich, P.K. Dorhout, J.M. Honig, J. Solid State Chem. 149 (2000) 3.
[2] C.N.R. Rao, J. Gopalakrishnan, New Directions in Solid State Chemistry. Structure Synthesis Properties Reactivity and Materials Design, Cambridge University Press, Cambridge, 1986.
[3] [a] J.L. Pizarro, M.I. Arriortua, L. Lezama, T. Rojo, G. Villeneueve, Solid State Ionics 63–65 (1993) 71;
[b] M.D. Marcos, P. Amoros, D. Beltran, A. Beltran, J.P. Atfield, J. Mater. Chem. 5 (1995) 71.
[4] G. Bonavia, J. DeBord, R.C. Haushalter, D. Rose, J. Zubieta, Chem. Mater. 7 (1995) 1995.
[5] [a] S. Fernandez, J.L. Mesa, J.L. Pizarro, L. Lezama, M.I. Arriortua, T. Rojo, Angew. Chem. Int. Ed. 41 (19) (2002) 2683;
[b] S. Fernandez, J.L. Mesa, J.L. Pizarro, J.S. Garitaonandia, M.I. Arriortua, T. Rojo, Angew. Chem. Int. Ed. 43 (8) (2004) 977;
[c] W.T.A. Harrison, M.L.F. Philips, T.M. Nenoff, J. Chem. Soc. Dalton Trans. 17 (2001) 2459;
[d] J. Liang, Y. Wang, J. Yu, Y. Li, R. Xu, Chem. Commun. 7 (2003) 882;
[e] W. Dong, G. Li, Z. Shi, W. Fu, D. Zhang, X. Chen, Z. Dai, L. Wang, S. Feng, Inorg. Chem. Commun. 6 (6) (2003) 776.
[6] [a] M. Ebert, L. Kaban, J. Less-Common Met. 81 (1) (1981) 55;
[b] C.Y. Ortiz-Avila, P.J. Squattrito, M. Shieh, A. Clearfield, Inorg. Chem. 28 (1989) 2608;
[c] M.D. Marcos, P. Gomez-Romero, P. Amoros, F. Sapiña, D. Beltran-Porter, R. Navarro, C. Rillo, F. Lera, J. Appl. Phys. 67 (9) (1990) 5998;
[d] M.P. Attfield, R.E. Morris, A.K. Cheetham, Acta Crystallogr. C 50 (1994) 981.

[7] J.L. Guth, H. Kessler, R. Wey, Stud. Surf. Catal. 28 (1986) 121.
[8] G.M. Sheldrick, SHELXS 97: Program for the Solution of Crystal Structures, University of Göttingen, Germany, 1977.
[9] G.M. Sheldrick, SHELXl 97: Program for the Refinement of Crystal Structures, University of Göttingen, Germany, 1977.
[10] P. Müller, R. Herbst-Irmer, A.L. Spek, T.R. Scheneider, M.R. Sawaya, Crystal Structure Refinement, Oxford University Press Inc., New York, 2006 57p..
[11] A.L. Spek, Acta Crystallogr. A 46 (1990) C34.
[12] J. Rodriguez-Carvajal, Rietveld Pattern Matching Analysis of Powder Patterns, 1994, unpublished.
[13] E. Dowty, ATOMS: A Computer Program for Displaying Atomic Structures, Shape Software, 512 Hidden Valley Road, Kingsport, TN, 1993.
[14] R.A. Brand, J. Lauer, D.M. Heralch, J. Phys. F: Mat. Phys. 13 (1983) 675.
[15] S. Alvarez, D. Avnir, M. Llunel, M. Pinsky, New. J. Chem. 26 (2002) 996.
[16] M. Llunel, D. Casanova, J. Cirera, J.M. Bofill, P. Alemany, S. Alvarez, M. Pinski, D. Yatumir, SHAPE v1.1a Program for Continuous Shape Measure Calculations of Polyhedral Xn and MLn Fragments, 2003.
[17] G.J. Long, A.K. Cheetham, P.D. Battle, Inorg. Chem. 22 (1983) 3012.
[18] A.G. Nord, Acta Chem. Scand. Ser. A 28 (1974) 150.
[19] C. Calvo, R. Faggiani, Can. J. Chem. 53 (1975) 1516.
[20] Y. Fei, In: T.J. Ahrens (Ed.), AGU Reference Shelf2: Mineral Physics and Crystallography—A Handbook of Physical Constants, AGU, Washington, 1995, pp. 29–44.
[21] M. Tsuboi, J. Am. Chem. Soc 79 (1957) 1351.
[22] Y. Tanabe, S.J. Sugano, Phys. Soc. Jpn. 9 (1954) 753.
[23] L.E. Orgel, J. Chem. Phys. 23 (1955) 1004.
[24] A.B.P. Lever, Inorganic Electronic Spectroscopy, Elsevier Science Publishers B.V., Amsterdam, Netherlands, 1984.